Transverse Flux Permanent Magnet Machines State of the Art and Design Procedure for Direct Drive Wind Turbines

Journal:	*IET Electric Power Applications*
Manuscript ID	EPA-2020-12-0103
Wiley - Manuscript type:	Original Research Paper
Date Submitted by the Author:	26-Dec-2020
Complete List of Authors:	Salehi, Maryam; Shahrood University of Technology, Electrical Engineering darabi, ahmad Ghaheri, Aghil; Shahid Beheshti University, Faculty of Electrical Engineering hoseintabar, mohamad;
Keywords:	wind turbines, permanent magnet generators, brushless machines, demagnetisation, energy conservation, synchronous generators
Abstract:	Transverse Flux machines offer a high torque and power density in low speed in which make them as promising choices for using in wind power plants. In this paper, the basic structure and capabilities of different types of TFMs are compared and then a comprehensive review on important features and operation characteristics of these machines are carried out in detail. In consequence, a new concentrated flux structure with a quiet large torque density and high power factor is presented that fully utilizes the PM consumption. Hence, the major crises of TFMs are attempted to downgrade for better exploitation of wind turbines. High efficiency, less PM eddy current and demagnetization, low leakage fluxes and low cogging torque are indicated by FEM results. A prototype is constructed and tested for the design procedure validation and the experimental results are in good agreement with FEM results

Transverse Flux Permanent Magnet Machines State of the Art and Design Procedure for Direct Drive Wind Turbines

Maryam Salehi[1], Ahmad Darabi[1], Aghil Ghaheri[2]✉, Mohammad Hoseintabar Marzebali[1]

[1] Shahrood University of Technology, Shahrood, Iran

[2] Shahid Beheshti University, Tehran, Iran

✉ *E-mail:* a_ghaheri@sbu.ac.ir

Abstract: Transverse Flux machines offer a high torque and power density in low speed in which make them as promising choices for using in wind power plants. In this paper, the basic structure and capabilities of different types of TFMs are compared and then a comprehensive review on important features and operation characteristics of these machines are carried out in detail. In consequence, a new concentrated flux structure with a quiet large torque density and high power factor is presented that fully utilizes the PM consumption. Hence, the major crises of TFMs are attempted to downgrade for better exploitation of wind turbines. High efficiency, less PM eddy current and demagnetization, low leakage fluxes and low cogging torque are indicated by FEM results. A prototype is constructed and tested for the design procedure validation and the experimental results are in good agreement with FEM results.

1. Nomenclature

B_{PM}	PM Magnetic flux density
Φ_{PM}	PM Magnetic flux
A_{PM}	PM active surface
ω_e	Angular velocity
p	Number of pole pairs
B_{Ag}	Average air-gap flux density
A	Surface current density
N	Number of turns per phase
D_g	Air-gap diameter
B_{FC}	Flux-concentrate's widths
H_{FC}	Flux concentrator's Axial height
B_{knee}	Material knee point Flux density
L_{PM}	PM's Axial height
K_{LF}	Leakage factor
K_{FF}	Focusing factor
ϕ_g	Air-gap linkage flux
f	Nominal frequency
S_n	Apparent power
b_{teeth}	Stator core's teeth width
h_{teeth}	Stator core's teeth axial height
A_s	Winding area
j	Current density
n_s	Rotor speed (*rpm*)
Φ_A	Peak flux of the stator cores when armature current acting alone and PMs flux is ignored
$\Phi_{PM,m}$	Peak flux of the stator cores when PMs act alone and armature current is zero.
A_{FC}	Flux-concentrator area next to the PMs
A_{PA}	Pole area
i	No. of U-shaped cores

2. Introduction

Over the past few decades, the energy generated by natural resources, especially wind power has been grown and different types of generators have been designed and manufactured in order to achieve high efficiency and low power losses. All types of wind turbine systems generally can be classified in three classes as follows [1] and [2]:

- ✓ Constant-speed with multi-stage gearbox and squirrel-cage induction generator with power level less than 1.5MW.
- ✓ Variable-speed with multi-stage gearbox contains standard doubly-fed induction generator (DFIG). The power levels of these type of generators is about 1.5 MW and the windings are fed by a low power rated converter.
- ✓ Variable speed direct-drive which has high energy yield, without gearbox failures and the low maintenance problems. The low-speed and high torque generators are fed by fully power electronic converters.

Constant-speed wind turbines have a simple structure and low-cost electrical parts. But, these structures suffer from high mechanical stress and low electrical power control. Variable-speed wind turbines resolve the major problems of constant-speed wind turbines. Among different types of variable-speed geared drive systems, doubly-fed induction generator systems are lightweight and low cost. However, the direct-drive generator systems seem to be more powerful in terms of energy yield, reliability and low copper losses compared to the geared drive systems. Among different types of direct-drive systems, the direct-drive permanent magnet synchronous generators are more attractive due to higher energy yield and lower power losses [3].

PM machines generally can be classified based on magnetic flux direction as radial flux permanent magnet machines (RFPMs), axial flux permanent magnet machines (AFPMs), and transverse flux permanent machines magnet (TFPMs).

RFPMs have simple structures, more robust than AFPM and TFPM machines and present the best performance in high speed applications[4].

AFPMs have a higher ratio of power to volume, short axial length and low cogging torque and noise especially in slotless machines compared to the RFPMs. However, these machines have a lower torque/mass, larger outer diameter, larger amount of PMs and structural instability in comparison with RFPMs. AFPMs, especially in large diameter to keep constant the air-gap, these machine should be designed with a heavy and strong structure [5]. Which makes them unsuitable for direct-drive wind turbines.

Compared to the RFPMs and AFPMs, TFPMs have low copper losses, short magnetic flux path, higher torque/mass and also lower cost/torque [5]. In low speed electrical machines, the copper losses are commonly higher than iron losses due to the high electrical loading. This unique feature gives TFPMs special characteristics such as high torque density, modular structure, simple winding and strong structure in short pole pitch and high pole number [6], [7], [8]. However, TFPMs with large air-gap has less efficiency and more expensive than other PM machines [9]. In TFPMs, magnetic and electrical loading set by the air-gap diameter and axial length of the machine, respectively. However, in RFPMs both magnetic and electrical loading depend on the air-gap diameter [10]. Each armature

core in TFPMs commonly is independent either electrically or magnetically from other cores, which enhances significantly the fault-tolerant capability[11].

General comparison on permanent magnet machines is given in TABLE 1. According to TABLE 1, TFPMs are the best choice for the low-speed high-torque direct-drive applications such as wind turbines [12], [13]. There is no particular reference which compare and analyze TFPMs in terms of structure and performance. Therefore, comparing and analyzing different types of TFPMs is necessary to choose the best structure, implement the appropriate design algorithm, and manufacture the appropriate generator for direct-drive wind turbine systems.

In this paper, after introduction, state of the art and important features of TFMs especially in wind power extraction are carried out in detail in section 3. Thus, the basic structure and operation principal of different types of TFMs are compared and classified to design an appropriate transverse flux generator for wind power applications. In section 4, important characteristics of TFPMs are fully described, compared and categorized. In section 5, the basic structure of the proposed generator is presented and a concentrated flux transverse flux permanent magnet generator (CF-TFPMG) with magnetic shunts is designed. The proposed structure has prominent features such as high efficiency, high torque density and power factor, low cogging torque and minimized PM eddy current and demagnetization, which are essential for direct drive wind generators. Afterwards, the proposed CF-TFPMG is prototyped and tested to validate the accuracy of the design process. The results proved that the proposed structure is well applicable in direct drive wind turbine applications.

3. TFPM Structure

TFMs are the kind of synchronous machines in which the flux path is perpendicular to the direction of the rotor rotation and current. TFMs have some privileged advantages such as modular structure in which each pair of poles usually forms a module. Hence, it offers some practical advantages such as feasible in-site assembly[14].

Since the introduction of the theory of TFMs, many changes have been made in the structure, and many structures have been introduced for TFMs which are compared and classified in this section. The main investigations are in the field of improving structures, increasing torque density, minimizing the leakage flux paths, increasing power factor and minimizing cogging torque and power losses.

In many cases, to improve the efficiency and cover the weaknesses of TFMs, these machines are usually combined with the structures of the other machines.

- Transverse flux synchronous reluctance machines (TFRM) [15].
- Transverse flux switched reluctance machines (TFSRM) [16].
- Transverse flux Switched reluctance with permanent magnet auxiliary poles (TFSRM)[17].
- Transverse flux–flux switching permanent magnet machines (TF-FSPM) [18]
- Transverse flux permanent magnet assisted reluctance machines (TFPMRM)[19].
- Transverse flux–flux reversal Machines (TF-FRM)[20]

As TFPMs do not have a unique and definite shape, classifying based on their appearance and structure is necessary. TFPMs can be classified based on their mover type, rotor, stator, winding, multi-phase and air-gap structures.

3.1. Mover Type

TFMs are divided into linear and rotary types based on their movement which are used in different industrial applications. Due to high force density and high efficiency, transverse flux permanent magnet linear machines (TFPMLM) are usually used in robotics and transportation industry [21]. In conventional TFPMLMs, the coil windings and PMs are commonly placed separately in primary and secondary. These types of machines cannot be economical in long transportation applications [22]. An effective approach to eliminate this problem would be locating PMs and coil on the short mover or stator sections. For this purpose, stator permanent magnet linear machines can be an alternative choice [23]. Stator permanent magnet machines can be divided into 1) flux reversal permanent magnet FRPMMs, 2) flux switching machines and 3) doubly salient machines. In FRPMs, the armature field is series with the magnetization direction which can lead to increase the risk of PM demagnetization [24]. Compared to the rotary types, TFPMLMs have low force density, low stability, the strong gravitational force between mover and stator, and the end effect force which limit the TFPMLMs performance [25], [26], [27], [28].

TABLE 1 COMPARISON BETWEEN CHARACTERISTICS OF AFPM, RFPM AND TFPM MACHINES

Quantity	RFPM	AFPM	TFPM
Advantages	✓ Simple structure ✓ more robust than AFPMs and TFPMs	✓ Low axial length to air-gap diameter ✓ Great surface active air-gap ✓ good heat transfer capability	✓ High torque density ✓ Low copper losses ✓ simple winding ✓ decoupled electric and magnetic loading ✓ higher torque/mass compare to AFPMs and RFPMs ✓ lower cost/torque compare to AFPMs and RFPMs
Drawbacks	✓ dependent electric and magnetic loading	✓ Heavy in large diameter ✓ dependence in electric and magnetic loading ✓ low power to mass ratio ✓ high copper losses	✓ Complicated structure (difficult assemblies) ✓ low power factor ✓ High torque ripple
Structure characteristics	✓ Null	✓ Short axial length	✓ strong structure in short pole pitch and high pole number
Best performance	✓ High-speed and high-torque applications	✓ High power to volume applications	✓ Low speed and high torque applications

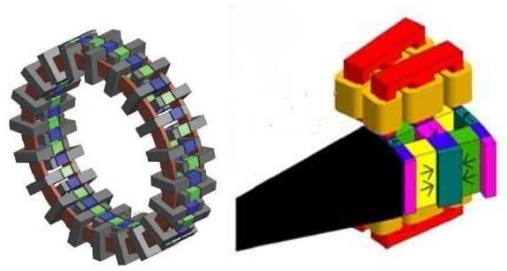

(a) (b)

Fig.1. *Winding scheme (a), Ring winding [29] (b), Pole winding [6]*

3.2. Rotor Structure

TFPMs can be classified based on rotor structure in different categories as follows:

- ✓ Ring-shaped or disc-shaped [4].
- ✓ Active or passive rotor structure [4].
- ✓ Inner rotor, outer rotor or sandwich rotor [4]
- ✓ Surface-mounted PMs, flux-concentrated, PM consequent pole, and Halbach array structure [6], [30], [31]

Ring-shaped rotor has a structure with nested cylinders and the air-gap surface is similar to the cylindrical shells. Therefore, the direction of the flux paths is radially in the air-gap. In disk-shaped rotor structures the air-gap surface is like a disk in which the direction of the flux paths is axially in the air-gap. Disk-shaped rotor structures have larger air-gap diameter and effective area air-gap, low air-gap reluctance and high torque density in comparison with the ring-shaped structures. However, in disk-shaped structures making lamination and setting air-gap are difficult.

In the active rotor structures, the rotor is supplied by PMs or coil windings which leads to generate excitation field. In the rotor passive structures does not exist excitation source on the rotor. However, stator should be synchronized with rotor which can be possible by means of reluctance torque, flux switching and flux reversal structures.

TFPMs with outer rotor structure are suitable for hub wheels in electric driven vehicles and hub wind-turbines [32]. In same magnet yield and volume, the outer rotor structures have lower coil resistance compared to the inner rotor structures [33]. In the equal air-gap diameter, the volume of the outer rotor structures is less than inner rotor structures. Therefore, outer rotor structures have more power density. However, the outer rotor topologies have more leakage flux between stator components, low power factor, complex structure and have a poorer heat transfer capability due to stay winding away from the air cooling [34]. In addition, it is possible to build TFPMs with double-rotor [29] and [35]. In [36] a TFPM machine with double-rotor structure and different speeds is designed.

The magnetization direction in PMs can be parallel to the air-gap (surface-mounted type) or perpendicular to the air gap (flux-concentrated type). The flux-concentrated type has lower leakage flux between stator cores and PMs. Therefore, flux-concentrated type has higher air-gap density compared to the surface-mounted type [37]. In flux-concentrated structures, the ferrite magnets can be easily used instead of rare-earth permanent magnets which are popular due to high cost and unavailability problems related to the rare-earth permanent magnets [38]. Although, ferrite magnets increase the weight of the machine.

Consequent structure is the combination of flux-concentrated and surface-mounted structures in which the flux paths are parallel to the air-gap and soft magnetic materials are used instead of adjoining PMs [30]. In these structures, the reluctance of the d and q axes is different. Therefore, consequent structures have high torque density and torque ripple compared to the surface-mounted structures.

Halbach array method is a kind of PM arrangement scheme in surface mounted structures to increase the magnetic flux density in the air-gap and decrease it in the back iron. Also, more sinusoidal flux distribution can be achieved by a precise design. One-sided flux characteristic in these structures leading to decrease the weight of the rotor yoke. Therefore, in the same magnet volume these structures offer a high torque density in comparison with other conventional structures. However, due to the large number of the magnet components with different charge directions, production and assembly costs increase significantly [31].

3.3. Stator Structure

TFPM machines can be classified based on stator structure in different classes as follows:

- ✓ Core shape including C-shaped, U-shaped, E-shaped, Z-shaped and claw pole.
- ✓ Core side including single sided and double sided.

In TFPMs with common U-shaped, C-shaped and E-shaped cores the stator pole pitch is twice of the rotor PM pole pitch. Some structures have been proposed such as Z-shaped cores or bidirectional cross-linking with special core shapes in which stator pole pitch is equal to the rotor PM pole pitch [39].

Z-shaped structures have less end winding, fringing flux, magnet leakage, and better thermal behavior than other conventional structures [40]. However, in Z-shaped structures making laminations and manufacturing process are difficult.

TFPMs with claw-pole cores have simple structures like the single-sided type in which the stator components are located on one side of the rotor, in addition these structures have high efficiency like double-sided structures [41]. However, making laminations in claw-pole cores is difficult or impossible.

TFPMs with double-sided stator structures use properly the space of the machine. These machines, furthermore, have higher power factor and output torque than single-sided structures. Double-sided structures reduce the high leakage flux in single-sided structures. However, double-sided types have complex structure which are only used in single-phase or double-phase mode [42]. On the other hand, single-sided structures can be designed in three-phase mode [32]. In both single-sided and double-sided structures, the winding can be classified into single turn or double turn per phase [4].

3.4. Winding Structure

TFPMs can be classified based on winding structure in different classes as follows:

- ✓ Ring winding
- ✓ Pole winding

Ring winding (toroidal winding) commonly known as the winding of TFPMs (Fig.1 (a)). Another type of the winding, which can be implemented in TFPMs is pole-winding which can be seen

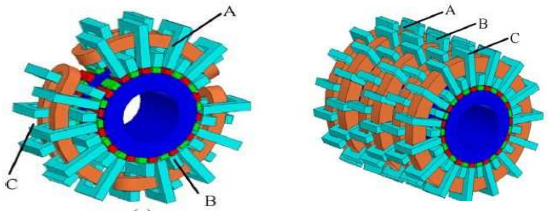

(a) (b)

Fig.2. *Three phase structure (a), Three phase arrayed in circumferential direction (b), Three phase arrayed in axis direction [39]*

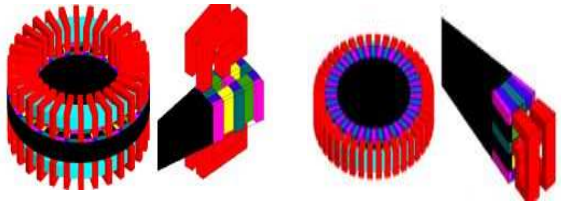

(a) (b)

Fig.3. *Air gap structure (a), Axial air gap (b), Radial air gap [6]*

in Fig.1 (b). There is no additional space for end winding in ring winding structures, and the half of the winding is inactive at any moment which can lead to increase the active weight of the machine. In TFPMs with ring windings, increasing the number of poles does not effect on the slot space of the winding. However, in pole winding structures, increasing the number of poles is not entirely independent from the slot space [37] and [43]. Also, TFPMs can be classified based on the number of windings in per phase to single or double winding [44]. In addition, new schemes have been proposed in recent papers to make the nominal torque and power flexible [45] and [46]. In [47], a new TFM with a semi-ring winding and E-shaped cores is proposed which has higher fill factor and lower copper weight than ring winding structures.

3.5. Multi-phase Structure

In order to have self-starting, better performance, and high reliability, multi-phase TFPMs are suggested. However, multi-phase TFPMs need a full-scaled inverter for each phase [48]. Two structures have been proposed for three-phase TFPMs, which can be generalized for more phases.

- ✓ Three phases arrayed along the circumferential direction
- ✓ Three phases arrayed along the axial direction

Three phase structure arrayed along the circumferential direction (Fig.2 (a)), has a runway-shaped winding, thus it needs additional space for end windings. Additional flux paths can lead to increase self-inductance and consequently decrease the power factor. Three phase structure arrayed along the axial direction (Fig.2 (b)), has toroidal winding and phases are fixed by one shaft [39]. The circumferential structures have fewer stator parts to produce the same torque. However, greater amount of coil windings is required in these structures. Therefore, each parts is heavier and larger than axial structures [49]. Imbalances of forces is one of the most important problems in circumferential structures which cause vibration and machine damage.

3.6. Air-gap Structure

There are two different type of air-gap structure in TFPMs as follows:

- ✓ Axial air gap (Fig.3 (a))
- ✓ Radial air gap (Fig.3 (b))

TFPMs with Radial air-gap are more common in single-sided structure. However, axial air-gap TFPMs should be designed in double-sided forms to avoid imbalance of the forces.

Fig.4 shows a comprehensive structure classification in TFPMs.

4. Important Features of TFPMs

4.1. High Torque Density

TFPMs have short magnetic flux paths and there is no any additional yoke in stator components. Therefore, TFPMs have a higher specific torque than other PM machines [50]. In TFPMs the torque density is directly related to the number of poles, electric and magnetic loading, the air-gap flux density, stator slot width and the weight of the materials.

a. High Pole Number

TFPMs are known as machines in which it is possible to increase the number of poles in constant volume to gain torque density [51]. TFPMs have homo-polar flux which causes an increase in the magnitude of the power by increasing the number of poles while the volume and the amount of the material are kept unchanged (same outer diameter, height, copper, irons) [52]. An increase in the number of poles in constant volume can lead to increase the rate of the flux variation and consequently torque density while the amount of linking flux is kept unchanged [53]. Increase in the number of poles leads to decrease the power factor because of the growth in the current and leakage flux [10] and [53]. Also, there are other factors which limits the number of poles including pole width and iron or copper losses [37]. Therefore, there should be a compromise between the pole number and power, power factor, cogging torque and efficiency.

b. Increasing Torque Density by Reducing Materials and Better Space Utilizing

TFPMs have modular structure and there is no extra stator yoke. Another method to provide the high torque density is better space utilization and mass reduction which make them particularly attractive for use in wind turbine generators [44].

To reduce the amount of the electromagnetic material, short magnetic flux paths can be an effective solution. This method is possible by decreasing the slot pitch and slot height.

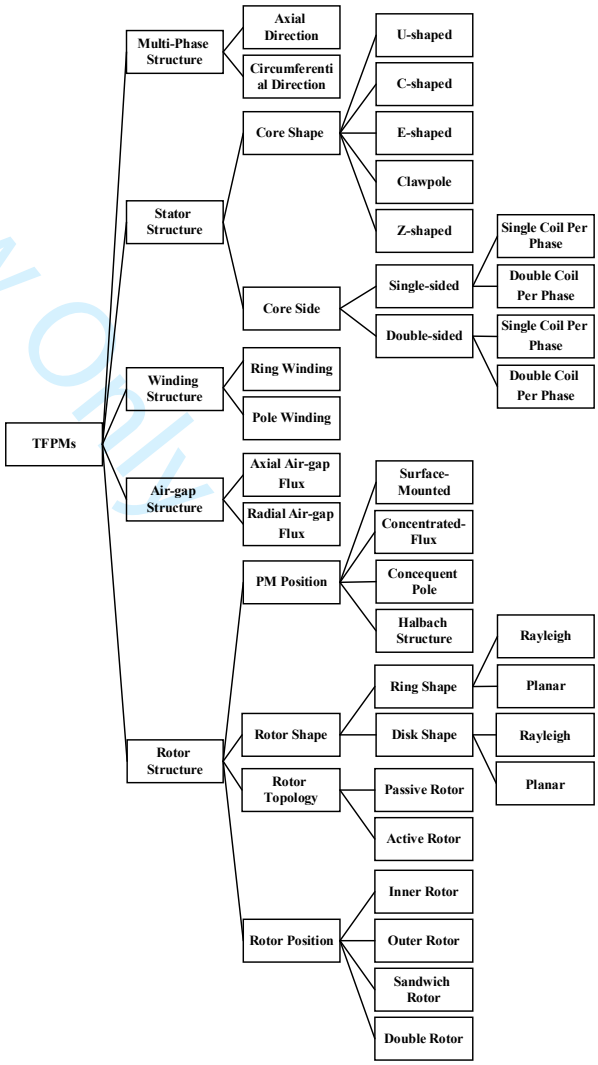

Fig.4. *TFPMs Structure*

TABLE 2 IMPORTANT FEATURES OF TFPMS, REASONS AND IMPROVEMENT

Features	Reasons	Improvement
High torque ripple	✓ The integrity in the number of rotor and stator poles ✓ modular structure ✓ High air-gap reluctance ✓ Magnetic flux distortion in air gap	✓ Increasing the number of stator and rotor poles ✓ Increasing the number of phases ✓ Modifying the shape of the rotor and stator poles ✓ Shifting and skewing methods ✓ Tooth pitching in rotor and stator cores ✓ Utilizing magnetic shunts ✓ Using Halbach array structures
Low power factor	✓ Leakage flux paths ✓ high rated current ✓ high phase inductance ✓ High magneto-motive force or electrical loading	✓ Improvement in the rotor and stator pole shape ✓ Utilizing magnetic shunts ✓ Using concentrated flux structures ✓ Small air-gap length ✓ Increasing the reluctance between two magnets ✓ Increasing the reluctance between two stator cores
High torque density	✓ homo-polar flux ✓ Separation of current and magnetic loading ✓ high pole number	✓ reducing the active materials ✓ Increasing the electric and magnetic loading ✓ Optimal No. of poles selection taking into account the leakage fluxes

This method is not applicable in AFPMs and RFPMs, since by decreasing the slot pitch the pole pitch decrease too. Plural module method decreases the width of the slots and stator teeth. However, by Plural module method leakage flux in the slot winding will increase[54]. To reduce the loss and weight of the TFPMs, the high-temperature superconducting (HTS) materials are used in [55]. In tubular transverse flux reluctance machine proposed in [56], utilizing spacers allows to minimize the mass. By reducing the weight of the machine, thermal considerations become more important as the machine components should be able to withstand the heat in operating temperature [57].

In common TFPMs, only half of the magnets helps to produce the back-EMF, and another half is inactive. These inactive magnets are required to produce a homo-polar flux in the cores around the winding. Some novel consequent-pole and fall back structures have been proposed in which the number of magnets is half of the common structures [30]. By increasing the ratio of the magnet thickness to the pole pitch the average force can be increased, however, this item is limited by core saturation effects and flux leakages.

c. Increasing electric and magnetic loading

In TFPMs the space required for winding and stator teeth is independent as by increasing the magnetic or electric loading, torque density can be increased without affecting each other [6]. High magnetic and electric loading are obtained by increasing the polar step and magneto-motive force, respectively. It is necessary to note that excessive increase in polar step and magneto-motive force leads to high active mass and poor power factor.

4.2. High Torque Ripple

TFPMs suffer from high cogging torque because of the high air-gap reluctance variation [58]. Also, cogging torque depends on the number and position of the rotor and stator cores [59]. In conventional TFPMs, the number of PMs are twice of the stator poles in per phase which causes considerable cogging torque. During the rotor rotation negative and positive cogging torque are created. Negative cogging torque creates when the magnetic flux attempts to pull the rotor against the direction of the motion and positive cogging torque generates when the magnetic flux attempts to pull the rotor in the direction of the motion [60].

Leakage flux in TFPMs has a considerable effect on the air-gap magnetic field. Therefore, it influences directly on electromagnetic force which causes torque ripple [61]. Moreover, small misalignments between phases especially in high pole numbers has a significant effect on cogging torque [62].The effects of different PM shapes on cogging force are investigated in [11]. An increase in the number of phases commonly minimizes the cogging torque [63]. Although, in many cases 5-phase machines have more torque ripple than 3-phase machines. By increasing the PM magnetization length and the height of the PMs, cogging torque can be increased like other PM machines [64] and [65]. In order to minimize the cogging torque, different methods have been proposed as follows:

- Increasing the number of rotor and stator poles [66]
- Modifying the shape of the rotor and stator poles [67]
- Stator and rotor skewing [68] and [69]
- Adjacent shift in the stator and rotor components within a phase [58] and [70]
- Utilizing magnetic shunts [71]
- Tooth pitching method in rotor or stator components [72]
- Utilizing Halbach-array PMs in rotor [73] and [74]

4.3. Low Power Factor

One of the most important drawbacks in TFPMs is low power factor which is due to 3-D complicated flux paths. Also, it is shown that the power factor can be decreased by increasing the rated current and phase inductance [75]. Another important reason to low power factor is higher magneto-motive force (MMF) or electrical loading. In this case, improvement in power factor can decline torque density [76]. Low power factor increases the voltage and current rates of the drive inverter [77]. Since the phases in TFPMs are electromagnetically independent, these machines only have self-inductance, however, if a small gap between phases in axial direction be considered, the mutual inductances cannot be neglected [58]. Also, a small gap between phases can lead to an imbalance between phases which is due to larger inductance in middle phase [34].

Estimating and minimizing leakage flux are important in the process of analyzing and designing electrical machines. Leakage flux can be classified into 1) no-load leakage flux which creates by PMs and 2) the armature reaction leakage flux [77]. Important no-load leakage fluxes in TFPMs are as follows:

1) When one magnet produces the linkage flux, the adjacent magnet fluxes leak from the sides (inactive magnets)

2) The leakage flux in the circumferential direction between adjacent magnets [77]

3) The leakage flux between two adjacent stator poles

4) End leakage flux in PMs [78]

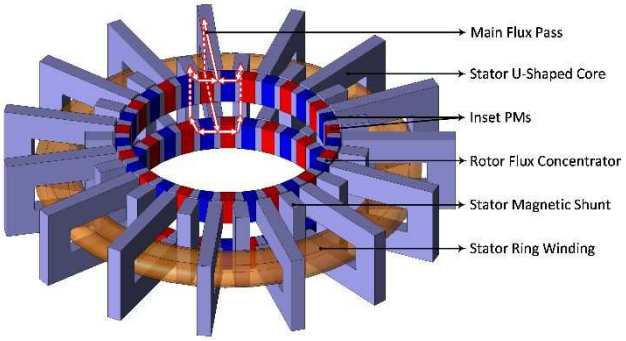

Fig.5. *One stack of CF-TFPMG*

Therefore, leakage flux reduction is an important key to increase the power factor without decreasing the mutual coupling between the stator and rotor poles in TFPMs [79]. The leakage fluxes between two magnets can be decreased by increasing the reluctance between two magnets or the reluctance between two stator cores [80]. By modifying the shapes of the poles, the flux deviation in the air-gap can be decreased [51], [27]. The magnetic shunts block the flux of the inactive magnets which is an effective solution to reduce the leakage fluxes in TFPMs. Many modern structures have been proposed to resolve the problem of inactive magnets. Double-sided stator structure or claw-pole stator cores are two simple methods to minimize the leakage fluxes in inactive magnets. In flux-concentrated structures, the leakage flux between the stator cores and the magnets is lower than surface-mounted structure. Also, an Increase in the number pole pairs can increase the leakage fluxes. In [81] to minimize the leakage flux, PMs are inserted into auxiliary rotor poles. The claw-pole cores can be axially shortened to minimize the armature leakage flux [82].

In Table2, a comprehensive classification of TFPMs based on important features is performed. According to the investigation in varies structures which is briefly illustrated in Table1 and Table2, this paper considers a TFPM machine with a simple structure, quite large torque density and low torque ripple.

5. CF-TFPMG Structure and Design

In this section a general design process is described. Design goal is to achieve a high torque density, low torque ripple and high power factor. Important characteristics such as PM demagnetization and power losses are carried out in next section.

5.1. Introducing Structure

Single phase of the CF-TFPMG is shown in Fig.5. Rotor consists of two rows of flux-concentrated PMs. PMs are magnetized in circumferential direction and PM magnetization direction is opposite to the adjacent PMs in each row. Also, magnetization direction in one of the rotor rows is opposite to another one with the same position. The outer stator type consists of magnetic shunts, U-shaped cores and ring winding. Ring winding is surrounded by U-shaped cores. Also, stator has module structure and the cores are easily laminated. Stator external type has an effective role in cooling the machines with high torque density. Magnetic shunts are used to decrease the leakage flux, decrease partial cancelation of the linkage flux, minimize torque ripple and increase the magnet usage. As it is shown in Fig.5, the magnetic flux of two adjacent PMs enters peripherally into the flux-concentrators and then it goes radially through the air-gap into the U-shaped cores. Next it passes via another row and magnetic shunts.

5.2. Design procedure

In this section, generator dimensions are designed and a general design process is illustrated in Fig.6. Due to optimal distance between stacks and optimal magnetic loading, the analytical calculations are simplified as follow:

- The saturation effects in iron cores are neglected
- The magnetic coupling between phases is considered zero

The apparent power for an electrical machine is given by:

$$S_n = m/T \int_0^T v(t).i(t)dt \quad (1)$$

$$S_n = m.V_{rms}.I_{rms} \quad (2)$$

Focusing factor has the direct effect on the average air-gap flux density. The focusing factor (K_{FF}) can be defined as:

$$K_{FF} = \frac{A_{FC}}{A_{PA}} \quad (3)$$

Based on different FEM simulations, the amount of the leakage flux can be estimated. By considering the leakage factor (K_{lf}), the average air-gap flux density is given by:

$$B_{AG} = K_{LF}.K_{FF}.B_{PM}\frac{l_{PM}}{b_{FC}} \quad (4)$$

The electric loading (A), can be represented as:

$$A = p\sqrt{2}I_{rms}N/\pi D_g \quad (5)$$

The no-load main magnetic flux (ϕ_T) in the U-shaped core is expressed as:

$$\phi g = iB_{AG}(2b_{FC} h_{FC})\cos(\omega_e t) \quad (6)$$

The peak of back-EMF is determined by:

$$V_{Peak} = N\frac{d\phi_g}{dt} = 2\pi f.NPB_{AG}(2b_{FC}h_{FC}) \quad (7)$$

Based on (5) and (7), the output power can be expressed as follow:

$$P_{out} = \eta.PF.mA\pi^2 fB_{AG}D_g(2b_{FC}h_{FC}) \quad (8)$$

According to the above equation, the three phase CF-TFPMG with 30 poles is designed. Table 3 lists the key dimensions and parameters of the designed CF-TFPMG.

6. FEM Analysis

3-D finite element method (FEM) is implemented to predict electromagnetic characteristics of the CF-TFPMG. Due to the 3-D flux paths, this machine can be simulated just in a 3-D scheme. One pole pair per phase is analyzed because of the magnetic periodicity of the machine. Due to the 3-D structure, extruded mesh is used in this paper which leads to minimize the number of element meshes

TABLE 3 PARAMETERS OF THE PROPOSED GENERATOR

Parameter	Data	Parameters	Data
Rated power	1 *kw*	Stator outer radios	141.5 *mm*
Rated current	1.5 *A*	Rotor inner radios	70 *mm*
Rated voltage	370 *V*	Rotor outer radios	80 *mm*
Air gap length	1.5 *mm*	Pole number	30
Axial length of the machine	250 *mm*	Rated speed	200 *rpm*
Stator inner radios	81.5 *mm*	Flux-concentrated width	6.5 *mm*
Axial height of the stator U-shaped core	70 *mm*	Stator slot height	30 *mm*
Stator core teeth width	10 *mm*	Number of turns per phase	225

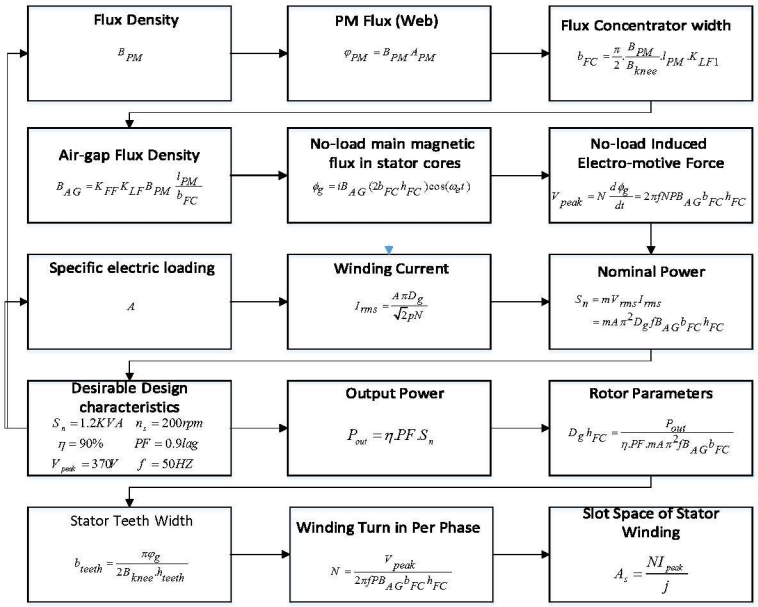

Fig.6. *General design process of the CF-TFPMG*

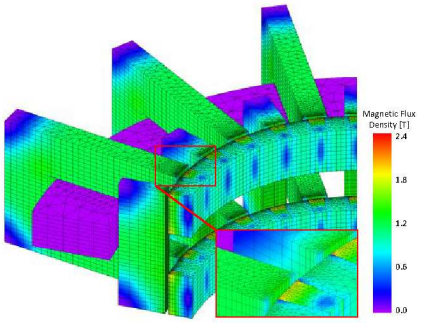

Fig.7. *3-D mesh model in one pole pair of CF-TFPMG*

while it has high accuracy. Partial 3-D meshed model including magnetic flux density distribution and flux paths in one pole pair are shown in Fig.7 and Fig.8, respectively. The linkage flux and voltage waveform at no-load condition are shown in Fig.9 (a) and Fig.9 (b), respectively. The sinusoidal back-EMF waveform indicates the accuracy of the design algorithm to achieve the sinusoidal linkage flux and voltage. The induced voltage and current waveforms, under full load condition are shown in Fig.9 (c) and Fig.9 (d).

6.1. Power Factor and Leakage Flux analysis

Due to leakage fluxes and core saturation the induced voltage is clearly reduced as against no-load condition which can lead to decrease the power factor. Optimal design of PMs and flux concentrators can minimize the leakage fluxes. As it is shown in Fig.10, the main path for the leakage fluxes occurred in region 1 and 2. Although, in 1, the leakage is almost constant in different loads thanks to PMs, but in 2, increasing the armature current leads to a non-negligible growth in undesirable fluxes. *Power factor can be evaluated by* [79]*:*

$$PF = \cos\left(\arctan\left(\frac{\varphi_a}{\varphi_{PM,m}}\right)\right) \quad (9)$$

According to (9), the value of the power factor for CF-TFPMG is 0.87 which is in an excellent level in transverse fluxes.

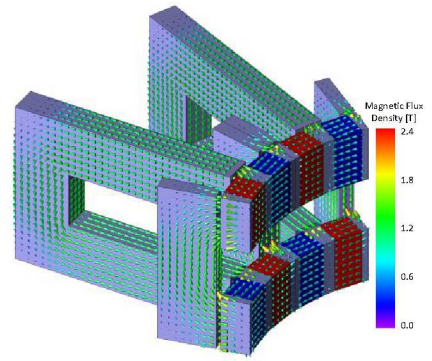

Fig.8. *Magnetic flux density and its direction in one pole pair of CF-TFPMG*

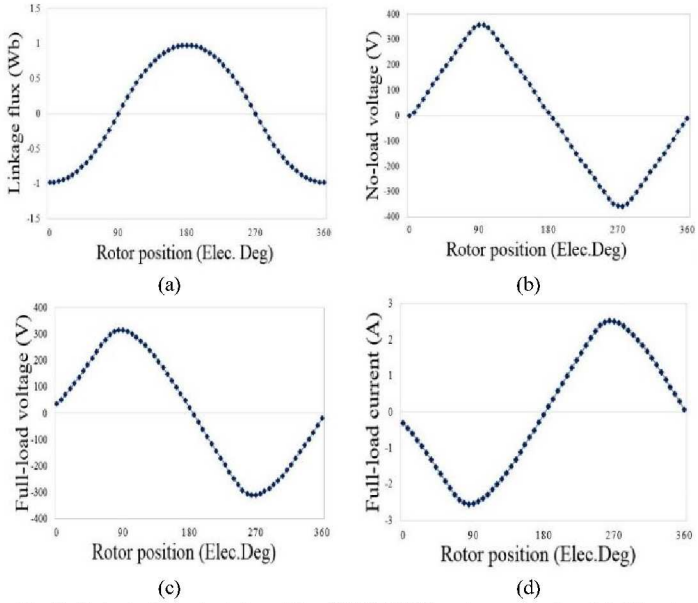

Fig.9. *Output characteristics of the CF-TFPMG under no-load and full load condition, (a), Total linkage flux at no-load condition (b), Back-EMF (c), Full load voltage (d), Full load current*

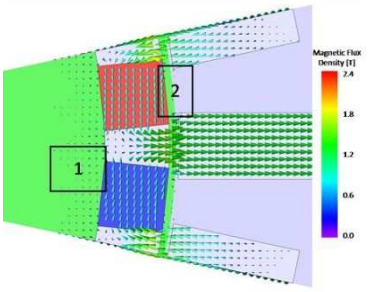

Fig.10. *Flux paths in TFPMG*

6.2. Cogging and Electromagnetic Torque Analysis

When CF-TFPMG rotates by constant speed, the average output electromagnetic torque is 49.38 Nm. The active weight (permanent magnets, iron cores and ring coil windings) is about 10.2 kg. Therefore, the torque density of CF-TFPMG is 4.83 Nm/kg. As it is shown in Fig.11 (a), three phase torque ripple is about 21%. Torque fluctuations resulted from current harmonics and electromagnetic field phase shift created by armature reaction may has a substantial impact on torque profile. But, in PM machines especially TFPMs, the main part of the torque ripple is usually due to the cogging torque effect. According to Fig.11 (b), more than 20% of the torque ripple is due to the cogging torque. Therefore, cogging torque suppression is necessary to improve torque ripple. It is necessary to note that in concentrated flux structures inherently the cogging torque is lower than surface mounted counterparts. Although the resulted torque profile is acceptable, aforementioned cogging torque reduction methods can be applied to achieve more smooth electromagnetic torque.

6.3. PM Demagnetization Analysis

Demagnetization of magnets is one of the reasons to decrease the motor performance. Thermal considerations are important in the process of electrical machine design in such a way that any increasing in the temperature can leads to PM demagnetization and injury to the different parts of the machine especially insulations. Therefore, the heat distributions calculation in some special machines chiefly in coil windings and magnets should be considered to design a coolant system. For this purpose, extracting the thermal network model can be an effective solution [83]. In [84], according to its application, a forced water cooling is used in a TFPM machine with claw-pole cores to prevent getting hot. To avoid increasing the temperature of the coil windings, windings are made up with hollow copper turns and heat sinked by utilizing water as a direct copper coolant [85].

Also, PM demagnetization can be happened from reverse coercive field as opposed to PM polarization. Furthermore, when the armature reaction flux is against the magnetization direction of the PMs, the risk of the demagnetization increases [72]. Another reason for this issue is low coercive force. The coercive force of the ferrite magnets is low which increases the risk of demagnetization in machines with ferrite magnets, but it has a reverse relation with heat

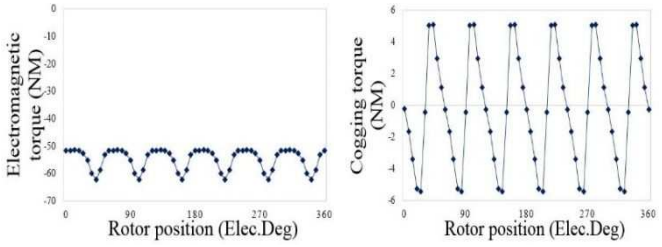

(a) (b)

Fig.11. *Torque characteristic of TFPMG, (a), Electromagnetic torque waveform under full load condition (b), Cogging torque waveform*

incensement and has a positive coefficient [86]. While, the thermal coefficient of coercively for NdFeB magnets is negative.

Proposed CF-TFPMG in this paper involves three important features which decreases the risk of the PM demagnetization; the large magnet thickness, using magnetic shunts and the flux concentrated structure that cover the PMs from air-gap flux. Based on evident, the possibility of demagnetization in CF-TFPMG without magnetic shunts is twice of the CF-TFPMG with magnetic shunts. Rare-earth magnets have a characteristic of large energy product, but it decreases when using in an area exceeding a knee point causing irreversible demagnetization. Large amounts of electric currents are run through an excitation coil where demagnetization may occur when a reverse magnetic field is applied on a magnet. The armature reaction flux and demagnetization ratio are illustrated in Fig.12 (a) and (b), respectively. As it is demonstrated, the risk of PM demagnetization at the edges of the PMs is high. As it can be seen from Fig.12 (a), the armature reaction flux only passes through the edge of PMs that faces the air-gap. The value of the flux is about 0.13 [T] and its direction is not in agreement with PM residual flux. Therefore, irreversible demagnetization occurred in these regions and its value is less than 20 percent. These parts are better to be filleted as it is considered for prototyping. Fig.13 shows magnetic field strength in PMs in different relative position of the stator poles. As it is clear, the coercive force in these regions is higher than its maximum level (800KA/m) which validate aforementioned statements.

6.4. Power Losses Analysis

The main goal in electrical machine design is to achieve high efficiency. Therefore, calculation of magnet, cores and copper losses are an important key in analyzing and designing electrical machines. Furthermore, the inactive parts like core holders can be important when there is significant leakage flux. Also, magnetic rotational loss is one of the most important losses in 3-D flux electrical machines which can be predicted accurately by 3-D time stepping finite element analysis. Utilizing Steel sheet laminations is an effective solution to minimize the eddy current losses in the stator and rotor cores.

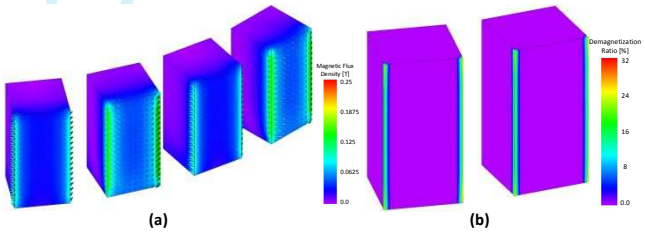

Fig.12. *Field demagnetization analysis (a) Armature reaction flux in PMs (b), PM Demagnetization in CF-TFPMG*

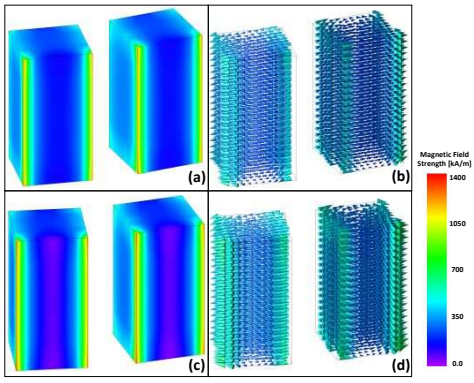

Fig.13. *Magnetic field strength distribution on PMs, (a)&(b) Stator poles are aligned with PMs, (c)&(d) Stator poles are unaligned with PMs*

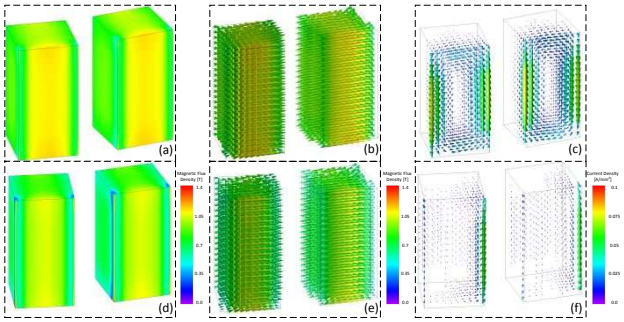

Fig.14. *Eddy loss analysis, (a)&(b), Magnetic flux density and (c), Eddy currents when stator poles are aligned with PMs, (d)&(e), Magnetic flux density and (f), Eddy currents when Stator poles are unaligned with PMs*

However, using steel sheet laminations is difficult and, in some cases, can make a problem for 3-D flux paths. The thickness, assembling and punching of laminations can influence on the core losses due to mechanical stresses. Therefore, the actual losses are more than the simulation losses. Compared to the steel sheet laminations, soft magnetic composite cores (SMC) have low core losses, simple manufacturing process and well conduct the flux in the 3-D paths [83]. In [87], in order to decrease losses, the hybrid stator is manufactured by the combination of silicon steel sheet laminations and SMC cores, and in [88], utilizing amorphous magnetic material in claw-pole stator cores is considered. However, SMC is a high cost material and has a high relative hysteresis loss.

In ferrite magnets due to high resistivity the magnet loss can be neglected. According to [12], dividing the magnets into more segments can reduce the magnet losses in rare-earth materials. However, this method causes some difficulties in the process of manufacturing and the length of the divided segments should be smaller than twice of the skin depth [89]. Core losses is zero if the magnetic flux does not change during the rotor rotation, so, the back iron is not required to be laminated.

In proposed structure, although the magnetic flux path of the machine has a 3-D form, the flux pass of each core segment pass through 2-D form. Therefore, all magnetic parts can be laminated and manufactured easily. Eddy currents in the PMs which are created by the harmonics of the stator cores, increase the magnet losses [90]. Fig.14 shows the magnetic flux density and eddy current in PMs, when the flux passes through the U-shaped cores are maximum and minimum. As it is shown, the eddy current at the edge of the PMs, near the air gap and flux concentrators are more than other places. In CF-TFPMG, the total power losses and efficiency in nominal are about 70W and 91%, respectively.

1. Experimental Results

The prototyped CF-TFPMG is constructed to confirm the correctness of the design procedure and FEM analysis. Rotor consists of the permanent magnets, flux-concentrators, shaft, non-magnetic holder (Fig.15 (a)) and spacing rings are shown in Fig.15 (d). Flux-concentrators are laminated in axial direction. To separate and fix the PMs on the rotor side, non-magnetic spacing rings are embedded. As it is shown in Fig.15 (e) stator consists of the stator cores, fiber glasses rings, ring windings, non-magnetic stator housing (Fig.15 (b)), non-magnetic spacers located between U-shaped cores, and magnetic shunts. The magnetic shunts and U-shaped cores are laminated in the radial direction which are fixed by fiber glasses rings. Silicon steel sheet laminations do not cause any problem for 3-D flux paths in both rotor and stator cores as mentioned in previous section. Stator components in each phase have 8 degrees mechanically clearance with one another. Two phases of the stator are shown in Fig.15 (c) and the prototyped CF-TFPMG is shown in

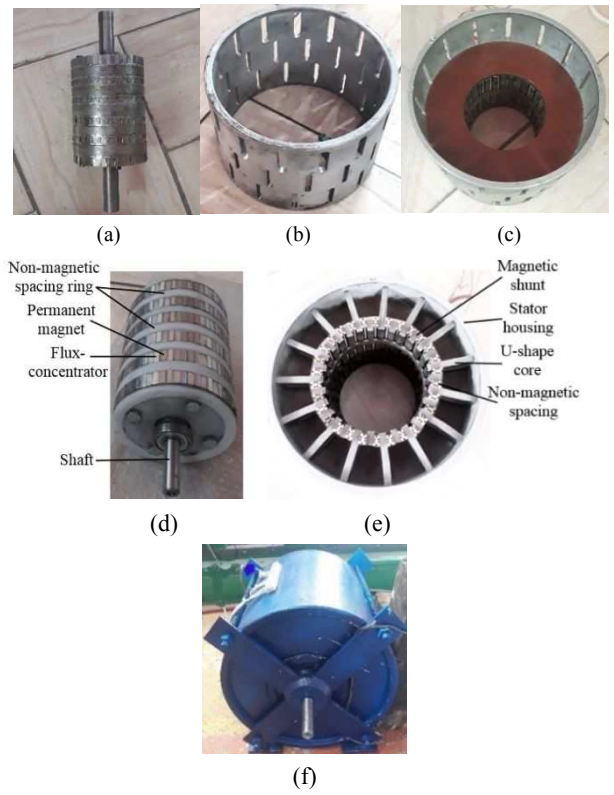

Fig.15. *Experimental platform, (a), Rotor holder (b), Stator housing (c), Two phase of the stator (d), Rotor structure (e), Stator structure (f), Prototyped CF-TFPMG*

Fig.15 (f). The experimental platform consists of a driver, a prime mover, the prototype, probes, multi-meter, tachometer, and oscilloscope. Fig.16 shows the no load test setup, when rotor rotates by the prime mover, the no-load back- EMF waveform at rated speed (200 rpm) is obtained (Fig. 17). As it is demonstrated in Fig.18, the experiment amplitude of fundamental no load back-EMF is 312V and the FEM simulation value is 334v. Therefore, the average error between the simulation and experimental results is about 7%, but, total error for the rms value of the harmonic waveform is less than 4 percent. The full-load set-up is similar to the no-load set-up with resistance load. In full-load condition the maximum efficiency is about 87%, that is so close to the predicted result. The voltage fundamental value is 278V and the FEM simulation value is 295V. The average error between the FEM results and measurement is about 6% (Fig.18). In 75% and 50% of the full load, the efficiency is decreased to 86% and 84%, respectively. As it was mentioned in previous section, cogging torque is one of the most important keys in the operation of wind turbine systems since this parameter has a direct impact on the starting toque especially in low wind speed. The peak of the measured cogging torque is about 6 NM. According to the Fig. 19, the error between the FEM result and measurement is about 12%. It is necessary to note that Measurement equipment errors must be considered.

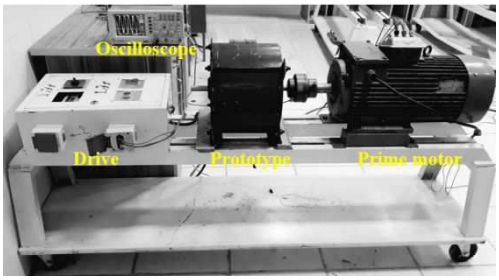

Fig.16. *Test bench of no-load condition*

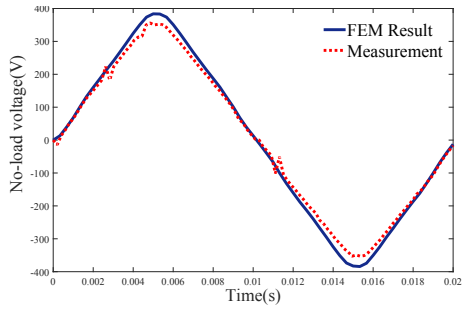

Fig.17. *Comparison of the measured and calculated no-load voltage in CF-TFPMG*

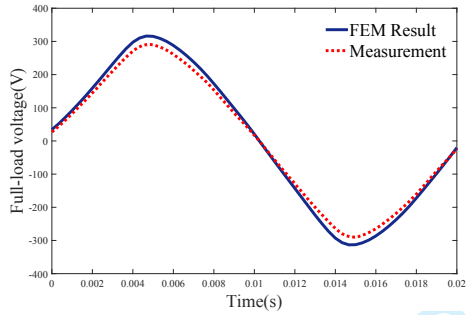

Fig. 18. *Comparison of the measured and calculated full load voltage in CF-TFPMG*

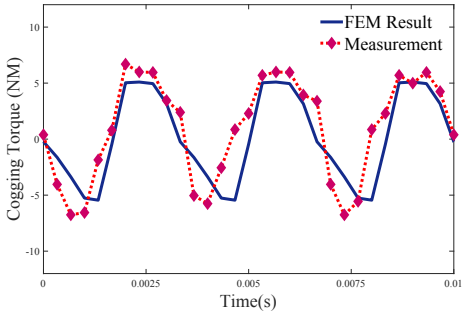

Fig. 19. *Comparison of the measured and calculated cogging torque in CF-TFPMG*

2. Conclusion

According to the comparisons between different permanent magnet machines, TFPM machines select as the best choice for the low-speed high torque applications especially in wind power generation. A comprehensive review on the structures and performance characteristics of TF machines has been performed. TFM features extracted and various methods are presented according to the authors comments to improve performance and reduce drawbacks. Then, by considering the important features of TFMs for wind turbines, a low speed concentrated flux transverse flux permanent magnet generator has been designed and tested. Based on results, characteristic of proposed structure is well fitted with wind generator necessities. The obtained full-load efficiency is near 90 percent and it has a torque density equal to 4.7 Nm/kg.

3. References

1. Polinder, H., et al., *Basic operation principles and electrical conversion systems of wind turbines.* Epe Journal, 2005. 15(4): p. 43-50.
2. Polinder, H., et al., *Comparison of direct-drive and geared generator concepts for wind turbines.* IEEE Transactions on energy conversion, 2006. 21(3): p. 725-733.
3. Bang, D.-j., et al., *Promising direct-drive generator system for large wind turbines.* EPE Journal, 2008. 18(3): p. 7-13.
4. Bang, D.-j., et al. *Comparative design of radial and transverse flux PM generators for direct-drive wind turbines. in 18th International Conference on Electrical Machines*. 2008. IEEE: p. 1-6.
5. Bang, D., et al. *Review of generator systems for direct-drive wind turbines*. in *European wind energy conference & exhibition, Belgium*. 2008: p. 1-11.
6. Husain, T., et al. *A comprehensive review of permanent magnet transverse flux machines for direct drive applications*. in *2017 IEEE Energy Conversion Congress and Exposition (ECCE)*. 2017. IEEE.
7. Hosseini, S., et al., *Design, prototyping, and analysis of a novel modular permanent-magnet transverse flux disk generator.* IEEE transactions on magnetics, 2010. 47(4): p. 772-780.
8. Shin, J.-S., et al. *Modeling and Prototype Experiments for a New High-Thrust, Low-Speed Permanent Magnet Synchronous Motor*. in *The 10th University of Tokyo-SNU Joint Seminar on Electrical Engineering*. 2010.
9. Bang, D.-J., et al. *Design of a lightweight transverse flux permanent magnet machine for direct-drive wind turbines*. in *2008 IEEE Industry Applications Society Annual Meeting*. 2008. IEEE.
10. Arshad, W., T. Backstrom, and C. Sadarangani. *Analytical design and analysis procedure for a transverse flux machine*. in *IEMDC. IEEE International Electric Machines and Drives Conference (Cat. No. 01EX485)*. 2001. IEEE: p. 115-121.
11. Fu, D., et al., *Presentation of a novel transverse-flux permanent magnet linear motor and its magnetic field analysis based on Schwarz–Christoffel mapping method.* IEEE Transactions on Magnetics, 2017. 54(3): p. 1-4.
12. Lundmark, S.T. and P.R. Fard, *Two-dimensional and three-dimensional core and magnet loss modeling in a radial flux and a transverse flux PM traction motor.* IEEE Transactions on Industry Applications, 2017. 53(3): p. 2028-2039.
13. Chen, A., R. Nilssen, and A. Nysveen, *Performance comparisons among radial-flux, multistage axial-flux, and three-phase transverse-flux PM machines for downhole applications.* IEEE Transactions on Industry Applications, 2010. 46(2): p. 779-789.
14. Cosic, A., C. Sadarangani, and J. Timmerman. *Design and manufacturing of a linear transverse flux permanent magnet machines*. in *2008 IEEE Industry Applications Society Annual Meeting*. 2008. IEEE.
15. Klöck, J. and W. Schumacher. *Modeling and control of transverse flux reluctance machines*. in *16th European Conference on Power Electronics and Applications*. 2014. IEEE: p. 1-10.
16. Du, J., P. Lu, and X. Yang. *Analysis and modeling of mutually coupled linear switched reluctance machine with transverse flux for wave energy conversion*. in *Eleventh International Conference on Ecological Vehicles and Renewable Energies (EVER)*. 2016. IEEE: p. 1-6.
17. Oh, J.-H. and B.-I. Kwon, *Design, optimization, and prototyping of a transverse flux-type-switched reluctance generator with an integrated rotor.* IEEE Transactions on Energy Conversion, 2016. 31(4): p. 1521-1529.
18. Lu, Q., et al., *Analysis of transverse-flux linear switched-flux permanent magnet machine.* IEEE Transactions on Magnetics, 2015. 51(11): p. 1-4.
19. Oh, J.-H., et al., *Analysis of a novel transverse flux type permanent magnet reluctance generator.* IEEE transactions on magnetics, 2014. 50(2): p. 809-812.
20. Kou, B., et al., *Modeling and analysis of a transverse-flux flux-reversal motor.* IEEE Transactions on Energy Conversion, 2016. 31(3): p. 1121-1131.
21. Zheng, P., et al., *Analysis and optimization of a novel tubular staggered-tooth transverse-flux PM linear machine.* IEEE Transactions on Magnetics, 2015. 51(11): p. 1-4.
22. Wang, Q., W. Huang, and D. Dong. *Force ripples suppression of tubular transverse flux and flux reversal linear permanent magnet motor based on ADRC*. in *20th International Conference on Electrical Machines and Systems (ICEMS)*. 2017. IEEE: p. 1-5.
23. Zhu, S., T. Cox, and C. Gerada. *Comparative study of novel tubular flux-reversal transverse flux permanent magnet linear machine*. in *2017 IEEE Energy Conversion Congress and Exposition (ECCE)*. 2017. IEEE.
24. Kou, B., et al., *Modeling and analysis of a novel transverse-flux flux-reversal linear motor for long-stroke application.* IEEE Transactions on Industrial Electronics, 2016. 63(10): p. 6238-6248.
25. Shin, J.-S., et al., *Transverse-flux-type cylindrical linear synchronous motor using generic armature cores for rotary machinery.* IEEE Transactions on Industrial Electronics, 2013. 61(8): p. 4346-4355.
26. Shin, J.-S., T. Koseki, and H.-J. Kim, *Proposal of double-sided transverse flux linear synchronous motor and a simplified design for maximum thrust in nonsaturation region.* IEEE transactions on magnetics, 2013. 49(7): p. 4104-4108.
27. Polinder, H., et al., *Conventional and TFPM linear generators for direct-drive wave energy conversion.* IEEE Transactions on Energy Conversion, 2005. 20(2): p. 260-267.
28. Ahmed, S., T. Koseki, and H.-J. Kim. *Detent force reduction for a novel transverse flux permanent magnet linear synchronous motor without compromising stroke length*. in *2017 11th International Symposium on Linear Drives for Industry Applications (LDIA)*. 2017. IEEE.
29. Lu, K. and W. Wu, *High torque density transverse flux machine without the need to use SMC material for 3-D flux paths.* IEEE Transactions on Magnetics, 2015. 51(3): p. 1-4.
30. Ueda, Y., et al., *Fundamental design of a consequent-pole transverse-flux motor for direct-drive systems.* IEEE transactions on magnetics, 2013. 49(7): p. 4096-4099.
31. Nasiri-Zarandi, R., A. Ghaheri, and K. Abbaszadeh, *Thermal Modeling and Analysis of a Novel Transverse Flux HAPM Generator for Small-Scale Wind Turbine Application.* IEEE Transactions on Energy Conversion, 2019. 35(1): p. 445-453.
32. Schmidt, E., *Finite element analysis of a novel design of a three phase transverse flux machine with an external rotor.* IEEE transactions on magnetics, 2011. 47(5): p. 982-985.

33. Kremers, M.F., J.J. Paulides, and E.A. Lomonova, *Toward accurate design of a transverse flux machine using an analytical 3-D magnetic charge model.* IEEE Transactions on Magnetics, 2015. 51(11): p. 1-4.
34. Ahmed, A. and I. Husain, *Power factor improvement of a transverse flux machine with high torque density.* IEEE Transactions on Industry Applications, 2018. 54(5): p. 4297-4305.
35. Zheng, P., et al., *Analysis and design of a transverse-flux dual rotor machine for power-split hybrid electric vehicle applications.* Energies, 2013. 6(12): p. 6548-6568.
36. Bomela, W., J.Z. Bird, and V.M. Acharya, *The performance of a transverse flux magnetic gear.* IEEE transactions on magnetics, 2013. 50(1): p. 1-4.
37. Husain, T., et al., *Design considerations of a transverse flux machine for direct-drive wind turbine applications.* IEEE Transactions on Industry Applications, 2018. 54(4): p. 3604-3615.
38. Wan, Z., et al. *A novel transverse flux machine for vehicle traction aplications*. in *2015 IEEE Power & Energy Society General Meeting*. 2015. IEEE.
39. Yang, G., et al., *Bidirectional cross-linking transverse flux permanent magnet synchronous motor.* IEEE transactions on magnetics, 2012. 49(3): p. 1242-1248.
40. Arshad, W.M., T. Backstrom, and C. Sadarangani, *Investigating a transverse flux machine with intermediate poles.* 2002.
41. Masmoudi, A., et al., *Optimizing the overlap between the stator teeth of a claw pole transverse-flux permanent-magnet machine.* IEEE Transactions on Magnetics, 2004. 40(3): p. 1573-1578.
42. Henneberger, G., et al. *On the parameters computation of a single sided transverse flux motor*. in *Workshop on Electrical Machines' Parameters, Technical University of Cluj-Napoca*. 2001.
43. Husain, T., et al., *Cogging torque minimization in transverse flux machines.* IEEE Transactions on Industry Applications, 2018. 55(1): p. 385-397.
44. Nica, F.V.T., K. Leban, and E. Ritchie. *Direct drive TFPM wind generator analytical design optimised for minimum active mass usage*. in *2013 8TH INTERNATIONAL SYMPOSIUM ON ADVANCED TOPICS IN ELECTRICAL ENGINEERING (ATEE)*. 2013. IEEE.
45. Husain, T., et al. *Winding schemes for wide constant power range of double stator transverse flux machine*. in *IEEE International Electric Machines & Drives Conference (IEMDC)*. 2015. IEEE: p. 1084-1091.
46. Aydin, E., et al. *A hybrid-excited axial transverse flux permanent magnet generator*. in *2016 IEEE Energy Conversion Congress and Exposition (ECCE)*. 2016. IEEE.
47. Husain, T., et al., *Design of a modular E-core flux concentrating transverse flux machine.* IEEE Transactions on Industry Applications, 2018. 54(3): p. 2115-2128.
48. Schuller, F., N. Parspour, and L. Chen. *Position control of a linear transverse flux machine with subordinate current control*. in *International Conference on Electrical Machines (ICEM)*. 2014. IEEE: p. 629-623.
49. Zhu, S., et al. *Comparative study and optimal design of alternative PM configuration transverse flux linear machine*. in *20th International Conference on Electrical Machines and Systems (ICEMS)*. 2017. IEEE: p. 1-6.
50. Liu, C., et al., *Design considerations of PM transverse flux machines with soft magnetic composite cores.* IEEE Transactions on Applied Superconductivity, 2016. 26(4): p. 1-5.
51. Dehlinger, N. and M.R. Dubois. *A new design method for the clawpole transverse flux machine. Application to the machine no-load flux optimization. Part I: Accurate magnetic model with error compensation*. in *The XIX International Conference on Electrical Machines-ICEM 2010*. 2010. IEEE: p. 1-7.
52. Ibala, A., et al., *A New Reluctance Model of a Claw Pole TFPM Using SMC for the Magnetic Circuit.* Ecologic Vehicles & Renewable Energies, Monaco, 2009.
53. Svechkarenko, D., J. Soulard, and C. Sadarangani. *A novel transverse flux generator in direct-driven wind turbines*. in *Proc. Nordic Workshop on Power and Industrial Electronics*. 2006.
54. Dreher, F. and N. Parspour. *A novel high-speed permanent magnet claw pole transverse flux machine for use in automation*. in *International Symposium on Power Electronics Power Electronics, Electrical Drives, Automation and Motion*. 2012. IEEE.
55. Keysan, O. and M.A. Mueller, *A transverse flux high-temperature superconducting generator topology for large direct drive wind turbines.* Physics Procedia, 2012. 36: p. 759-764.
56. Popa, D.-C., et al., *Optimized design of a novel modular tubular transverse flux reluctance machine.* IEEE transactions on magnetics, 2013. 49(11): p. 5533-5542.
57. Jordan, S. and N.J. Baker. *Design and build of a mass critical, air-cooled transverse flux machine for aerospace*. in *XXII International Conference on Electrical Machines (ICEM)*. 2016. IEEE: p. 1453-1458.
58. Liu, C., et al., *Cogging torque minimization of SMC PM transverse flux machines using shifted and unequal-width stator teeth.* IEEE Transactions on Applied Superconductivity, 2016. 26(4): p. 1-4.
59. Patel, M.A. and S.C. Vora, *Analysis of a fall-back transverse-flux permanent-magnet generator.* IEEE Transactions on Magnetics, 2017. 53(11): p. 1-5.
60. Masmoudi, A. and A. Elantably. *A simple assessment of the cogging torque in a transverse flux permanent magnet machine*. in *IEMDC. IEEE International Electric Machines and Drives Conference (Cat. No. 01EX485)*. 2001. IEEE: p. 754-759.
61. Wang, W., H. Wang, and H. Shen. *Analysis of electromagnetic force and vibration characteristics for transverse flux permanent magnet motor*. in *Chinese Control and Decision Conference (CCDC)*. 2016. IEEE: p. 6929-6934.
62. Washington, J., C. Pompermaier, and G. Atkinson. *Robust electromagnetic design of Transverse Flux Machines for high volume production*. in *XXII International Conference on Electrical Machines (ICEM)*. 2016. IEEE: p. 877-883.
63. Schmidt, E., *3-D finite element analysis of the cogging torque of a transverse flux machine.* IEEE transactions on MAGNETICS, 2005. 41(5): p. 1836-1839.
64. Zou, J., Q. Wang, and Y. Xu, *Influence of the permanent magnet magnetization length on the performance of a tubular transverse flux permanent magnet linear machine used for electromagnetic launch.* IEEE Transactions on plasma science, 2010. 39(1): p. 241-246.
65. Baserrah, S. and B. Orlik. *Comparison study of permanent magnet transverse flux motors (PMTFMs) for in-wheel applications*. in *International Conference on Power Electronics and Drive Systems (PEDS)*. 2009. IEEE: p. 96-101.
66. Dobzhanskyi, O., R. Gouws, and E. Amiri. *Comparison analysis of PM transverse flux outer rotor machines with and without magnetic shunts*. in *2016 IEEE Energy Conversion Congress and Exposition (ECCE)*. 2016. IEEE.
67. Pompermaier, C., et al. *Reduction of cogging torque in transverse flux machines by stator and rotor pole shaping*. in *2016 IEEE Energy Conversion Congress and Exposition (ECCE)*. 2016. IEEE.
68. Jia, Z., et al., *Cogging torque optimization of novel transverse flux permanent magnet generator with double C-hoop stator.* IEEE Transactions on Magnetics, 2015. 51(11): p. 1-4.
69. Ueda, Y., et al., *Cogging-torque reduction of transverse-flux motor by skewing stator poles.* IEEE Transactions on Magnetics, 2016. 52(7): p. 1-4.
70. Nasiri-Zarandi, R. and A.M. Ajamloo. *Implementation of PM Step Skew Technique to Optimum Design of a Transverse Flux PM Generator for Small Scale Wind Turbine*. in *2019 IEEE Milan PowerTech*. 2019. IEEE.
71. Ueda, Y., et al., *Small cogging-torque transverse-flux motor with magnetic short circuit under unloaded condition.* IEEE Transactions on Magnetics, 2014. 50(11): p. 1-4.
72. Wan, Z. and I. Husain. *Design, analysis and prototyping of a flux switching transverse flux machine with ferrite magnets*. in *2017 IEEE Energy Conversion Congress and Exposition (ECCE)*. 2017. IEEE.
73. Nasiri-Zarandi, R., A. Ghaheri, and K. Abbaszadeh. *Cogging torque reduction in U-core TFPM generator using different Halbach-array structures*. in *2018 International Symposium on Power Electronics, Electrical Drives, Automation and Motion (SPEEDAM)*. 2018. IEEE.
74. Nasiri-Zarandi, R., A.M. Ajamloo, and K. Abbasazdeh, *Design Optimization of a Transverse Flux Halbach-Array PM Generator for Direct Drive Wind Turbines.* IEEE Transactions on Energy Conversion, 2020.
75. Anglada, J.R. and S.M. Sharkh, *An insight into torque production and power factor in transverse-flux machines.* IEEE Transactions on Industry Applications, 2017. 53(3): p. 1971-1977.
76. Yu, Z. and C. Jianyun. *Power factor analysis of transverse flux permanent machines*. in *International Conference on Electrical Machines and Systems*. 2005. IEEE: p. 450-459.
77. Lu, K., P.O. Rasmussen, and E. Ritchie, *Design considerations of permanent magnet transverse flux machines.* IEEE Transactions on Magnetics, 2011. 47(10): p. 2804-2807.
78. Xia, J., et al., *Analysis on axial end flux leakage and resonance characteristic of TFPM linear generator for thermoacoustic electric generation system.* IEEE Transactions on Magnetics, 2016. 52(12): p. 1-7.
79. Anpalahan, P., J. Soulard, and H.-P. Nee. *Design steps towards a high power factor transverse flux machine*. in *Proc. European Conf. on Power Electronics and Applications*. 2001.
80. Yan, H., et al. *Research on a novel tubular transverse-flux permanent-magnet linear machine for free-piston energy converter*. in *International Conference on Electrical Machines and Systems*. 2011. IEEE: p. 1-5.
81. Oh, J.-H. and B.-I. Kwon, *Improved transverse flux type permanent magnet reluctance generator with auxiliary rotor pole inserted permanent magnet.* IEEE Transactions on Magnetics, 2014. 50(11): p. 1-4.
82. Guo, Y., et al., *Parameter Computation and Performance Prediction of a Claw Pole/Transverse Flux Motor with Soft Magnetic Composite Core.* Journal of Science, Technology and Engineering, 2007.
83. Lei, G., et al., *Multidisciplinary design analysis and optimization of a PM transverse flux machine with soft magnetic composite core.* IEEE Transactions on Magnetics, 2015. 51(11): p. 1-4.
84. Darabi, A., A. Sarreshtehdari, and H. Tahanian. *Design of the forced water cooling system for a claw pole transverse flux permanent magnet synchronous motor*. in *21st Iranian Conference on Electrical Engineering (ICEE)*. 2013. IEEE: p. 1-5.
85. Doering, J., G. Steinborn, and W. Hofmann, *Torque, power, losses, and heat calculation of a transverse flux reluctance machine with soft magnetic composite materials and disk-shaped rotor.* IEEE Transactions on Industry Applications, 2014. 51(2): p. 1494-1504.
86. Mohammadi Ajamloo, A., K. Abbaszadeh, and R. Nasiri-Zarandi, *A Novel Transverse Flux Permanent Magnet Generator for Small-Scale Direct Drive Wind Turbine Application: Design and Analysis.* Scientia Iranica, 2019.
87. Dubois, M.R., et al. *Clawpole transverse-flux machine with hybrid stator*. in *Proc. Int. Conf. on Electrical Machines (ICEM2006)*. 2006.
88. Dehlinger, N. and M.R. Dubois. *Clawpole transverse flux machines with amorphous stator cores*. in *18th International Conference on Electrical Machines*. 2008. IEEE: p. 1-6.
89. Yamazaki, K. and A. Abe, *Loss investigation of interior permanent-magnet motors considering carrier harmonics and magnet eddy currents.* IEEE Transactions on Industry Applications, 2009. 45(2): p. 659-665.
90. Nagarkatti, A., O. Mohammed, and N. Demerdash, *Special losses in rotors of electronically commutated brushless dc motors induced by non-uniformly rotating amature MMFS.* IEEE Transactions on Power Apparatus and Systems, 1982(12): p. 4502-4507.